

# Magnetic anisotropy and crystalline texture in BaO(Fe<sub>2</sub>O<sub>3</sub>)<sub>6</sub> thin films deposited on GaN/Al<sub>2</sub>O<sub>3</sub>

P. R. Ohodnicki,<sup>a)</sup> K. Y. Goh, Y. Hanlumuang, K. Ramos, and M. E. McHenry  
*Materials Science and Engineering, Carnegie Mellon University, Pittsburgh, Pennsylvania 15213*

Z. Cai and K. Ziemer  
*Chemical Engineering Department, Northeastern University, Boston, Massachusetts 02115*

H. Morkoc and N. Biyikli  
*Department of Electrical and Computer Engineering, Virginia Commonwealth University, Richmond, Virginia and Physics Department, Virginia Commonwealth University, Richmond, Virginia 23284*

Z. Chen, C. Vittoria, and V. G. Harris  
*Department of Electrical and Computer Engineering, Northeastern University, Boston, Massachusetts 02115*

(Presented on 10 January 2007; received 31 October 2006; accepted 19 December 2006; published online 11 May 2007)

BaO(Fe<sub>2</sub>O<sub>3</sub>)<sub>6</sub> (BaM) thin films were deposited by pulsed laser deposition on GaN/Al<sub>2</sub>O<sub>3</sub> substrates. A pole figure obtained from the (006) reflection indicated that ~81% of the film volume had the *c* axis tilted less than 5° from the film normal. A low anisotropy field was inferred from vector coil vibrating sample magnetometer (VVSMM) measurements. The reduction in *H<sub>a</sub>* from literature values and a two-step switching of the easy axis magnetization is postulated to result from interdiffusion and misalignment effects. To alleviate interdiffusion and to improve the *c*-axis alignment, experiments were repeated with lower deposition temperatures, thinner films, and MgO buffer layers. The features of the hysteresis loop due to two-step switching and the in-plane coercivity were reduced while the anisotropy field (*H<sub>a</sub>*) was larger. Films deposited with MgO buffer layers are observed to have single-step switching of the easy axis magnetization, larger anisotropy fields, and sharp ferromagnetic resonance (FMR) peaks. Films with MgO buffer layers were determined to have anisotropy fields *H<sub>a</sub>*=1.57 T by FMR and *H<sub>a</sub>*~1.5–1.6 T as determined from the difference in the saturation fields for the easy and hard axis loops. © 2007 American Institute of Physics. [DOI: 10.1063/1.2712295]

Barium hexaferrite, BaO(Fe<sub>2</sub>O<sub>3</sub>)<sub>6</sub>, is a technologically important material for microwave device applications. A *c*-axis easy magnetization direction (EMD) normal to the film is crucial for propagating electromagnetic waves.<sup>1</sup> Sharp ferromagnetic resonance (FMR) requires small dispersion in the orientation of the easy axes. Integration of high frequency BaO(Fe<sub>2</sub>O<sub>3</sub>)<sub>6</sub> materials with wide band gap semiconductor materials such as SiC and GaN for device applications<sup>2,3</sup> is a current goal of the microwave ferrite research community.

BaO(Fe<sub>2</sub>O<sub>3</sub>)<sub>6</sub> has the magnetoplumbite crystal structure with the *P6<sub>3</sub>/mmc* space group and lattice constants *a* = 0.5892 nm and *c* = 2.3183 nm, respectively.<sup>4</sup> This hexagonal structure gives rise to uniaxial magnetocrystalline anisotropy with the magnetic easy axis parallel to the *c* axis.<sup>5</sup> A large magnetocrystalline anisotropy contributes to a large anisotropy field and large FMR absorption frequency. The FMR linewidth in these materials is directly related to the dispersion of the *c*-axis orientations in the films. Here, we discuss the magnetic properties and alignment of the easy axes in BaO(Fe<sub>2</sub>O<sub>3</sub>)<sub>6</sub> thin films deposited on GaN with and without MgO buffer layers.

*M*-type BaO(Fe<sub>2</sub>O<sub>3</sub>)<sub>6</sub> (BAM) films were deposited on GaN by pulsed laser deposition (PLD) in 20 mtorr of oxygen

at 920 °C. The GaN substrate was 1.0 μm thick and grown on sapphire by metal organic chemical vapor deposition (MOCVD). The epilayer of the first BaM/GaN films were 0.4 μm thick with the *c* axis oriented normal to the film surface. A *c*-axis (001) oriented GaN single crystal was used to facilitate the *c*-axis texture in the BaO(Fe<sub>2</sub>O<sub>3</sub>)<sub>6</sub> film. Films were annealed for 3–6 min to reduce dislocation density and porosity. A second series of 250 nm thick films was grown with and without a 25 nm MgO buffer layer separating the hexaferrite film from the GaN substrate. These films were grown at a lower substrate temperature (880 °C).

The orientation of the hexaferrite crystals with respect to the substrate was determined by x-ray diffraction (xrd) 2θ scans as well as x-ray pole figures. XRD 2θ scans were taken using Cu *Kα* radiation. Pole figures were taken using a Philips high resolution x-ray diffractometer. The magnetic properties of the resulting films were characterized by vibrating sample magnetometry (VSM) and vector coil torque magnetometry.

Figure 1(a) shows a typical x-ray diffraction pattern for a BaO(Fe<sub>2</sub>O<sub>3</sub>)<sub>6</sub> film grown without a buffer layer on a GaN/Al<sub>2</sub>O<sub>3</sub> substrate. The hexaferrite diffraction peaks are all indexed to (002*l*) reflections. This indicates the orientation relationship between the hexaferrite grains and the *c* axis normal to the GaN surface.

Figure 1(b) shows BaO(Fe<sub>2</sub>O<sub>3</sub>)<sub>6</sub> texture as determined

<sup>a)</sup>Electronic mail: pohodnic@andrew.cmu.edu

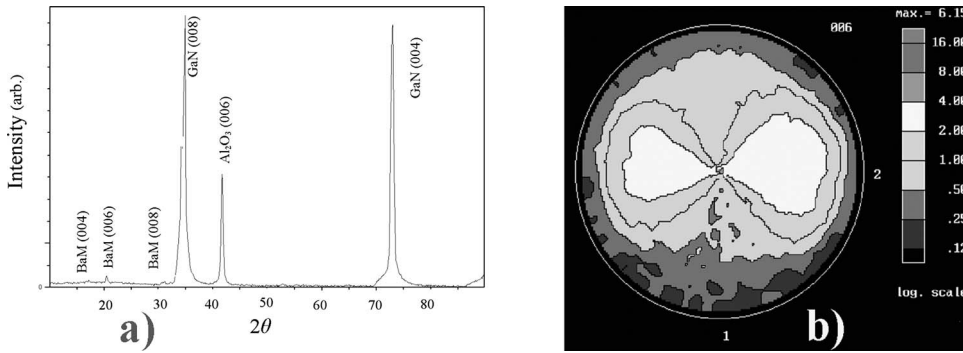


FIG. 1. (a) X-ray diffraction patterns for a  $\text{BaO}(\text{Fe}_2\text{O}_3)_6$  film on  $\text{GaN}/\text{Al}_2\text{O}_3$  without a buffer layer. Known diffraction peaks are indexed. (b) (006) pole figure of  $\text{BaO}(\text{Fe}_2\text{O}_3)_6$  film. The legend for the contours is shown on the right with 1.0 indicating random orientation. Scans were done in every  $2.5^\circ$  angular grid.

from pole figure data. The pole figures of the (006) peaks are shown. Strong intensity at the center of the pole figure indicates that most grains are oriented with their  $c$  axes normal to the film surface. This texture has been previously reported for  $\text{BaO}(\text{Fe}_2\text{O}_3)_6$  films that were grown on 6H-SiC and alumina substrate.<sup>2,3</sup> Analysis of the pole figure for the first sample ( $\text{BaM}/\text{GaN}/\text{Al}_2\text{O}_3$  high deposition  $T$ ) indicates that  $\sim 81\%$  of the film volume had the  $c$  axis tilted less than  $5^\circ$  from the film normal. The volume fraction ( $X_v$ ) of the film whose grains are oriented close to the film normal have been calculated from the peak intensities of the x-ray pole figure by angular integration.

Figure 2 shows a comparison of (006) pole figures of  $\text{BaO}(\text{Fe}_2\text{O}_3)_6$  films: (a) thicker films deposited on GaN (same as Fig. 1(b)), (b) 250 nm thick films deposited at  $880^\circ\text{C}$  on GaN, and (c) 250 nm thick films deposited at  $880^\circ\text{C}$  with a 25 nm MgO buffer layer on GaN. A less desirable texture is clearly observed for the high temperature deposited  $\text{BaM}/\text{GaN}$  film. For reduced thicknesses (250 nm), lower deposition temperatures, and use of the MgO buffer layer, the  $c$ -axis dispersion is reduced.

For as-grown films with a MgO buffer layer ( $\text{BaM}/\text{MgO}/\text{GaN}$ ), a magnetization  $4\pi M_s = 0.34$  T was measured for a loop exhibiting an easy axis coercivity,  $H_c = 0.12$  T. For the hard axis loops (in plane), the coercivities appear to decrease dramatically for the lower deposition temperatures and MgO buffer layer samples due to the improved  $c$ -axis texturing. Anisotropy fields  $H_a$  have been determined by fitting the Kittel equation for the observed FMR frequency  $\omega$ :

$$\frac{\omega}{\gamma} = H_{\text{eff}} = H_{\text{ext}} + H_a - 4\pi M_s, \quad (1)$$

in an external field  $H_{\text{ext}}$  where the gyromagnetic ratio  $\gamma = 2.8 \times 2\pi \times 10^6$  Hz/Oe. For as-deposited  $\text{BaM}/\text{MgO}/\text{GaN}$  thin film a FMR frequency of  $\omega = 56 \times 2\pi \times 10^9$  Hz has been

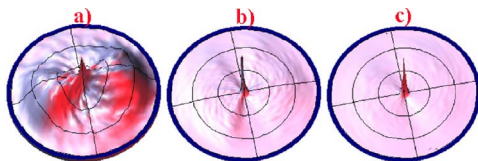


FIG. 2. (Color online) Comparison of (006) pole figures of  $\text{BaO}(\text{Fe}_2\text{O}_3)_6$  films: (a) thicker films deposited on GaN. (b) 250 nm thick films deposited at  $880^\circ\text{C}$  on GaN, and (c) 250 nm thick films deposited at  $880^\circ\text{C}$  with a 25 nm MgO buffer layer on GaN.

measured in an external field  $H_{\text{ext}} = 7.735$  K. Using the measured value of  $4\pi M_s$ , an anisotropy field  $H_a = 1.57$  T is inferred.

For the same  $\text{BaM}/\text{MgO}/\text{GaN}$  film a FMR linewidth of 0.071 T was measured. Using Eq. (1) it is clear that the FMR linewidth  $\Delta\omega \sim \Delta H_a$  if there are no significant fluctuations in the sample magnetization. Figure 3(a) shows a scanning electron microscopy (SEM) micrograph of an as-deposited  $\text{BaM}/\text{GaN}$  film and a cartoon showing dispersion of the  $c$  axes from the direction of the film normal. Although they are not shown here for brevity, SEM images of the  $\text{BaM}/\text{GaN}$  samples prepared at lower deposition temperatures and with MgO buffer layers show a smooth surface, indicating a better film quality. Figure 3(b) shows the geometry used for easy and hard axis magnetization measurements and the rotation axis for torque magnetometry.

Demagnetization corrected easy and hard axis hysteresis loops are shown in Figs. 4(a) and 4(b) for the films grown without a buffer layer. For these films, an anisotropy field of  $H_a \sim 0.9$ – $1.1$  T for the high deposition temperature and  $H_a \sim 1.3$ – $1.5$  T for the low deposition temperature is inferred. A two-step switching of the magnetization is observed in the easy axis loop. This is presumably due to incomplete  $c$ -axis texturing and Ga and N interdiffusion. Similar data for  $\text{BaM}/\text{MgO}/\text{GaN}$  films are shown in Fig. 4(c). For these films a single-step easy axis loop and a significantly larger anisotropy field are inferred from the hysteresis loops ( $H_a \sim 1.5$ – $1.6$  T). If it is assumed that the demagnetization factor can be approximated by that of an oblate spheroid, an average aspect ratio can be inferred from the shearing of the easy axis loops. For the  $\text{BaM}/\text{MgO}/\text{GaN}$  film an aspect ratio of  $\sim 6$  was inferred for a demagnetization factor of approximately 9.5–10 (cgs). Since this value is less than  $4\pi$ , grain

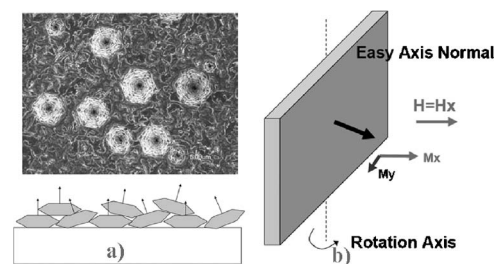


FIG. 3. (a) SEM micrograph of as-deposited  $\text{BaM}/\text{GaN}$  (002) film and a cartoon showing dispersion of the  $c$  axes from the direction of the film normal. (b) Schematic of geometry of vector VSM for torque magnetometry of perpendicular films.

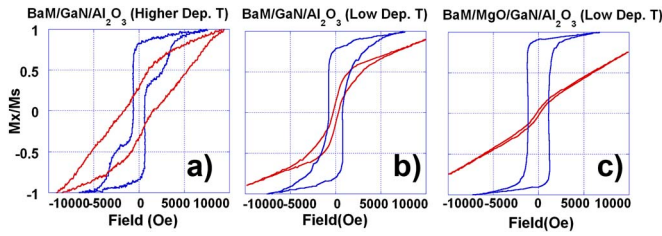


FIG. 4. (Color online) (a) Easy and hard axis magnetization curves and components of the magnetization ( $M_y$ ) normal to the applied field for the high deposition temperature BaM/GaN (002) film (b) for the low deposition temperature BaM/GaN (002) film, and (c) for a BaM/MgO/GaN (002) film.

shape may play a role in determining the demagnetization factor in addition to the overall film geometry.

Torque magnetometry was performed using a Lakeshore vector coil VSM. By measuring the magnetization component normal to the applied field, the torque exerted on the sample by the magnetic anisotropy can be determined.<sup>6</sup> For a thin film sample with mirror symmetry in the film plane one can use two perpendicular sets of coils since the  $z$  component of the magnetization,  $M_z$ , can be taken as 0 by symmetry ( $\tau_{\text{Zeeman}} = \tau_{\text{anisotropy}} = M_y H$ ) (Fig. 3(b)). An expansion of the uniaxial magnetocrystalline anisotropy with a correction for demagnetization:

$$E = -K_1 \text{crystal} \sin^2(\theta - \theta_0) - K_2 \text{crystal} \sin^4(\theta - \theta_0) + \dots + 2\pi\Delta N M_s \sin^2(\theta - \theta_0), \quad (2a)$$

can be differentiated with respect to  $\theta$  and used to fit torque data as a function of rotation angle,  $\tau(\theta)$ . In this case, fits of the torque data were made to an expression of the following form under the assumption that the  $K_1$  term of the crystalline anisotropy is dominant and accounting for the fact that the condition  $H \gg H_a$  is not satisfied:<sup>7</sup>

$$\tau(\theta) = T_0 + T_1 \sin[2(\theta - \theta_0)] + T_2 \sin[4(\theta - \theta_0)] + T_3 \sin[6(\theta - \theta_0)] + \dots \quad (2b)$$

Figure 5(a) illustrates a comparison of  $\tau(\theta)$  data, in a field of 1 T, for the BaM/GaN and BaM/MgO/GaN films deposited at the lower deposition temperature. The angular dependence of the torque was fitted to Eq. (2b) where  $\theta - \theta_0$  is the angle between the film normal orientation and the field. For the BaM/GaN film, the effective first order anisotropy constant for the film without demagnetizing field corrections was estimated to be  $K_1 = T_1 = 0.37 \times 10^6$  erg/cm<sup>3</sup> and for the BaM/MgO/GaN film the corresponding value was estimated to be much larger,  $K_1 = T_1 = 1.04 \times 10^6$  erg/cm<sup>3</sup>. Using a demagnetizing field correction as in Eq. (2a) with  $\Delta N$  taken from the shearing of the easy axis hysteresis loops, an estimate for the  $K_1$  of the BaM/MgO/GaN film due only to the effective crystal anisotropy of the film is obtained to be  $K_{1\text{crystal}} = 1.36 \times 10^6$  ergs/cm<sup>3</sup>. The calculated anisotropy field using the value of  $K_{1\text{crystal}}$  is  $H_a = 2K_{1\text{crystal}}/M_s = 1.01$  T for the BaM/MgO/GaN film which is smaller than inferred from FMR and easy and hard axis magnetization curves but significantly larger than the corresponding values estimated for the films without a MgO buffer layer. Disagreement be-

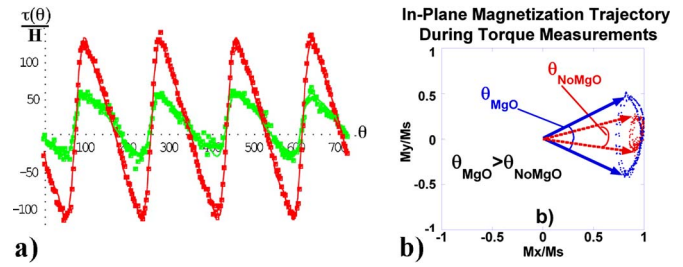


FIG. 5. (Color online) (a) Comparison of  $M_y(\theta) = \tau(\theta)/H$  data for a BaM/GaN and for a BaM/MgO/GaN film fitted to Eq. (2b) and (b) magnetization trajectory for the BaM/MgO/GaN film.

tween quantitative values using other techniques is presumed to be related to the demagnetization corrections assumed, the implicit assumption of in-plane mirror symmetry with respect to the plane of rotation of the film normal, and primarily the fact that the maximum fields that can be employed were not sufficient to completely saturate the sample along the hard axis. Even for a pure uniaxial anisotropy, the assumption that  $K_1 = T_1$  is only true if the applied field during the rotation experiment is significantly larger than the anisotropy field of the sample. In fact, the maximum applied fields that can be used here are actually smaller than the anisotropy field estimated from extrapolation of hard axis  $M-H$  loops ( $H < H_a$ ). The significant deviation of  $M$  from the field direction can be seen in Fig. 5(b) where the magnetization trajectories are shown throughout the torque measurements for the two different samples deposited at 880 °C while rotating the sample in a fixed field of  $H = 1$  T. The relatively large angle swept out by the magnetization vector for the BaM/MgO/GaN sample shows that the anisotropy field for this sample is the largest and that the condition  $H \gg H_a$  is not satisfied here.

Crystallographic texture was improved, a higher anisotropy field was achieved, and a lower in-plane (hard axis) coercivity was observed in BaM/GaN/ $\text{Al}_2\text{O}_3$  thin films by depositing thinner films (250 nm thickness BaM) at lower deposition temperatures (880 °C) and, in particular, by using a MgO buffer layer (BaM/MgO/GaN/ $\text{Al}_2\text{O}_3$ ). Two-step switching in the easy axis hysteresis loops is eliminated using a MgO buffer layer and a sharp FMR linewidth is obtained. Torque magnetometry using a vector VSM clearly supports the larger effective values of  $K_u$  and  $H_a$  for the BaM/MgO/GaN samples as compared to the samples without a MgO buffer layer.

One of the authors (P.R.O.) gratefully acknowledges funding through a National Defense Science and Engineering Graduate Research Fellowship (NDSEG). This work was funded by NSF Grant No. DMR-0406220. This work was also supported in part by the Army Research Laboratory and was accomplished under Cooperative Agreement No. W911NF-04-2-0017.

<sup>1</sup>J. D. Adam *et al.*, IEEE Trans. Microwave Theory Tech. **50**, 721 (2002).

<sup>2</sup>Y. Chen *et al.*, Appl. Phys. Lett. **88**, 062516 (2006).

<sup>3</sup>Z. Chen *et al.*, J. Magn. Magn. Mater. **301**, 166 (2006).

<sup>4</sup>E. Pollert, Prog. Cryst. Growth Charact., **11**, 155 (1985).

<sup>5</sup>J. H. Smit and P. J. Wijn, *Ferries* (Wiley, New York, 1959), p. 194.

<sup>6</sup>K. Ouchi and S. Iwasaki, IEEE Trans. Magn. **24**, 3009 (1988).

<sup>7</sup>E. Secemski, J. Phys. D **3**, 1770 (1970).